ISUOG VIRTUAL INTERNATIONAL SYMPOSIUM 2021

State-of-the-art Ultrasound Imaging in Obstetrics and Gynecology

17-18 April 2021

REGISTER NOW ▸

Using ultrasound together with other technologies to improve the lifelong health of women and babies

- Two streams of scientific content over two days, delivered through the ISUOG virtual platform which will exceed your expectations
- A mixture of lectures and practical, interactive training, including scan demonstrations, pattern recognition sessions and case report discussion
- Leading international and local experts in obstetrics, gynecology and imaging
- Live program delivered from 7:30 - 18:30 Calgary, Canada time (Mountain Daylight Time)
- Content available on Demand, at a time, pace and location to suit you until 17 May 2021
- All non-member registration fees include a 12-month ISUOG basic membership

Provisional program

Sessions will run simultaneously, providing two streams of content both days.

Highlights include:

- Obstetrics: the first trimester, beyond the routine mid-trimester fetal ultrasound scan, screening to improve pregnancy outcomes, fetal growth and health, ultrasound in labor, and more
- Gynecology: ectopic pregnancy, miscarriage, endometriosis, menopause, ovarian tumors, tubal and uterine pathology, and more
- Special sessions include advanced imaging/MRI, fetal therapy and COVID

The symposium will be co-chaired by:

Jo-Ann Johnson (Canada),
Denise Pugash (Canada)

Symposium Advisory Group

Shabnam Bobdiwala (UK)
George Condous (Australia)
Karen Fung-Kee-Fung (Canada)
Jon Hyett (Australia)
Simon Meagher (Australia)
Liona Poon (Hong Kong)
Angela Ranzini (USA)
Magdalena Sanz Cortes (USA)

Who should attend?

This interactive course is designed for Maternal Fetal Medicine (MFMs), OB-GYNs, Radiologists, Sonographers, Geneticists, Researchers, Trainees/ Residents and other maternity care providers. The program will appeal to a wide global audience, with a focus on North American educational needs.

See you ONLINE in 2021! For more information, please visit:
isuog.org/event/17th-isuog-international-symposium.html

isuog.org

Ultrasound Obstet Gynecol 2019; **54**: 207–214
Published online in Wiley Online Library (wileyonlinelibrary.com). **DOI:** 10.1002/uog.20120

Hindbrain morphometry and choroid plexus position in differential diagnosis of posterior fossa cystic malformations

D. PALADINI[1], G. DONARINI[1], S. PARODI[2], G. VOLPE[1], G. SGLAVO[3] and E. FULCHERI[4]

[1]*Fetal Medicine and Surgery Unit, IRCCS Istituto Giannina Gaslini, Genoa, Italy;* [2]*Epidemiology and Biostatistics Unit, IRCCS Istituto Giannina Gaslini, Genoa, Italy;* [3]*Department of Obstetrics and Gynecology, University Federico II, Naples, Italy;* [4]*Fetopathology Unit, IRCCS Istituto Giannina Gaslini, Genoa, Italy*

KEYWORDS: Blake's pouch cyst; Dandy–Walker malformation; fetus; posterior fossa; three-dimensional ultrasound; vermian hypoplasia

ABSTRACT

Objective *To assess the differential diagnostic significance of a series of quantitative and qualitative variables of the cerebellar vermis in fetuses with posterior fossa cystic malformation, including Dandy–Walker malformation (DWM), vermian hypoplasia (VH) and Blake's pouch cyst (BPC).*

Methods *This was a retrospective study of confirmed cases of DWM, VH and BPC, diagnosed at the Fetal Medicine and Surgery Unit of the Federico II University between January 2005 and June 2013 or the Fetal Medicine and Surgery Unit of G. Gaslini Hospital between July 2013 and September 2017. All included cases had good-quality three-dimensional (3D) volume datasets of the posterior fossa, acquired by transvaginal ultrasound through the posterior fontanelle. The midsagittal view of the posterior fossa was the reference view for the study. We assessed brainstem–tentorium angle and brainstem–vermis angle (BVA), as well as craniocaudal (CCVD) and anteroposterior (APVD) vermian diameters and vermian area (VA), which were normalized by biparietal diameter (BPD) to take into account gestational age (CCVD/BPD × 100, APVD/BPD × 100 and VA/BPD × 100, respectively). Finally, the position of the fourth ventricular choroid plexus (4VCP) was defined as normal ('up') or abnormal ('down'), relative to the roof/cyst inlet of the fourth ventricle.*

Results *We analyzed 67 fetuses with posterior fossa malformations (24 cases of DWM, 13 of VH and 30 of BPC). The mean gestational age at diagnosis was 23.6 weeks. Regardless of gestational age, the BVA differed significantly between the three groups, and the VA/BPD was able to differentiate between VH and BPC. In differentiating between VH and BPC, the greatest areas under the receiver–operating characteristics curve were those for VA/BPD ratio. The 4VCP position was down in all cases of DWM and VH, while it was up in all cases of BPC.*

Conclusions *Our data support the concept that VA/BPD ratio and 4VCP position may be used to differentiate between DWM, VH and BPC in the fetus. In our series, the position of the 4VCP had the highest accuracy, but a larger number of VH cases should be evaluated to confirm that an up position of the 4VCP indicates BPC while a down position indicates DWM or VH. Copyright © 2018 ISUOG. Published by John Wiley & Sons Ltd.*

INTRODUCTION

Cystic anomalies of the posterior fossa include Dandy–Walker malformation (DWM), vermian hypoplasia (VH), Blake's pouch cyst (BPC), megacisterna magna and arachnoid cyst. The criteria employed to diagnose and differentiate between them prenatally vary considerably, and very few studies take into consideration the appearance and position of the fourth ventricular choroid plexus (4VCP)[1]. Of the five cystic malformations, the most relevant in clinical terms and in terms of prognosis are probably DWM, VH and BPC. However, they may share certain imaging features, especially in prenatal life, and in the fetus their differential diagnosis may be difficult, with relatively frequent disagreement between imaging techniques, including ultrasound and magnetic resonance imaging (MRI), and pathologic assessment[1–4]. The series published so far underscore this, with a relatively high rate of false positives and incorrect diagnoses[1,3–5]. Furthermore, dissection of the posterior fossa often alters the relationship between the various tissues, due to leakage of the cerebrospinal fluid, with consequent potential for diagnostic mistakes at necropsy[5].

The aim of this study was to assess the differential diagnostic significance of a series of quantitative and

Correspondence to: Prof. D. Paladini, Fetal Medicine and Surgery Unit, Istituto G. Gaslini, Genoa, Italy (e-mail: dpaladini49@gmail.com)

Accepted: 24 August 2018

qualitative variables of the cerebellar vermis in cases of posterior fossa cystic malformation, including DWM, VH and BPC.

METHODS

This was a retrospective study of fetuses with DWM, VH and BPC diagnosed at two institutions between 2005 and 2017 (Fetal Medicine and Surgery Unit, Department of Obstetrics and Gynecology, Federico II University, January 2005–June 2013; Fetal Medicine and Surgery Unit, G. Gaslini Hospital, July 2013–September 2017) and retrieved from the hospitals' databases. Inclusion criteria were: (1) gestational age confirmed by a first-trimester scan; (2) prenatal sonographic diagnosis of one of the following: DWM, VH, BPC; (3) availability of one or more good-quality three-dimensional (3D) volume datasets of the posterior fossa, acquired by transvaginal ultrasound imaging, as described below; (4) confirmation of the diagnosis by postmortem examination or neonatal MRI.

All cases had undergone 3D transvaginal neurosonography[6] using a GE Voluson 730 Expert, E8 or E10 (GE Healthcare Ultrasound, Milwaukee, WI, USA) ultrasound machine and a 5–9-MHz or 6–12-MHz volumetric transducer, according to the gestational age at the time of neurosonography. In each case, one or more 3D volume datasets had been acquired through the posterior fontanelle. This ensures high resolution and allows multiplanar image correlation analysis.

For the purposes of this study, each volume dataset was processed offline using a dedicated software package (4D View, version 17.1, GE Healthcare Ultrasound). Multiplanar image correlation with volume contrast imaging (1 mm slice thickness) was used as the reference visualization mode, and the midsagittal view of the fetal posterior fossa, obtained after alignment in three orthogonal planes, was used as the reference view. The following anatomic measurements were obtained from each dataset (Figure 1): brainstem–tentorium angle, brainstem–vermis angle (BVA), as well as craniocaudal (CCVD) and anteroposterior (APVD) vermian diameters and vermian area (VA). Because the latter three parameters increase linearly with advancing gestation[7], they were normalized by biparietal diameter (BPD) to take into account gestational age (CCVD/BPD × 100, APVD/BPD × 100 and VA/BPD × 100, respectively). Finally, the position of the 4VCP was defined as normal ('up') or abnormal ('down'), relative to the roof/cyst inlet of the fourth ventricle.

The CCVD was measured from the edge of the culmen to the edge of the uvula, according to Malinger *et al.*[7]; in cases of VH, the maximum CCVD that could be visualized was considered. Using multiplanar image correlation, the position of the 4VCP was classified as superolateral (up) or inferolateral (down) in relation to the fourth ventricular roof or to the inlet of the cystic structure evaginating from the fourth ventricle (Figure 2). This was achieved by positioning the reference marker at the posterior edge of the vermis in the midsagittal image, and then assessing the position of the 4VCP in the corresponding coronal

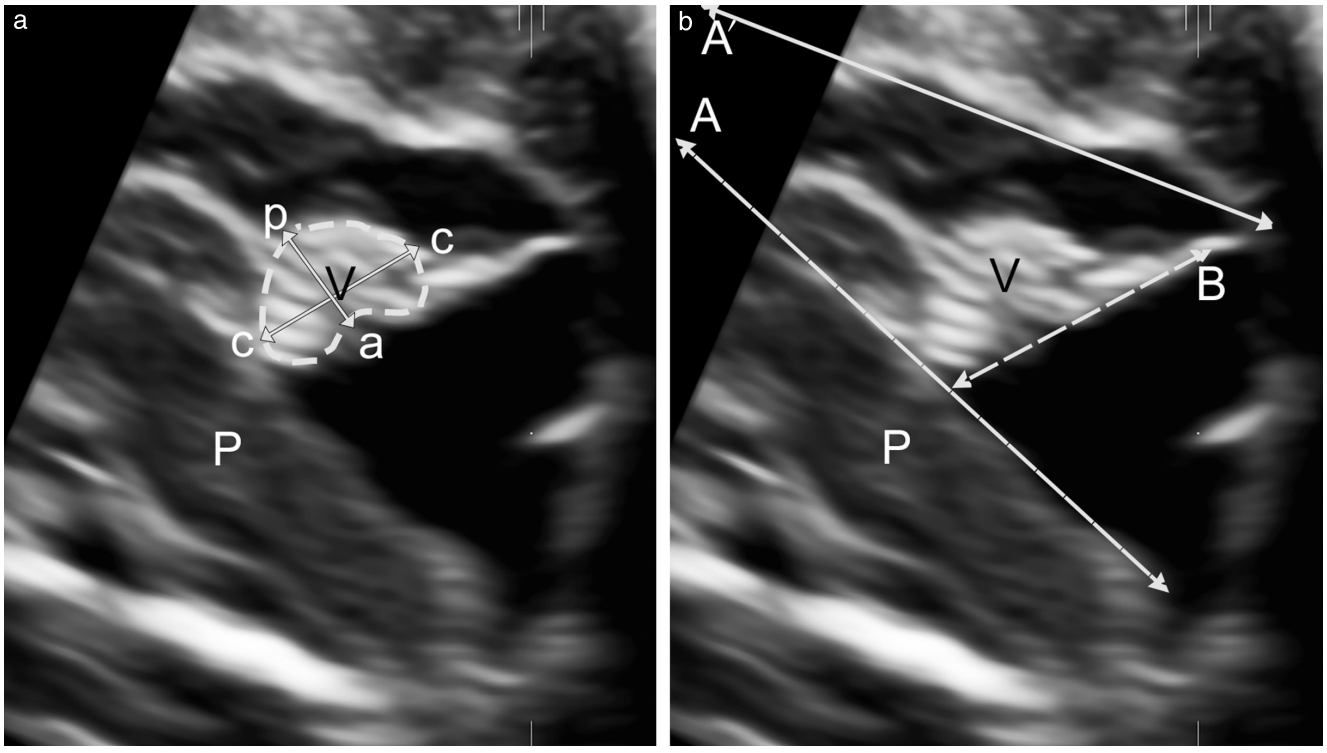

Figure 1 Measurements on transvaginal neurosonography of vermis and posterior fossa in 21-week fetus with Blake's pouch cyst. (a) Craniocaudal (c–c) and anteroposterior (a–p) vermian diameters are indicated by arrows, and vermian area by dashed line. (b) Brainstem–tentorium angle is angle between line A, drawn along posterior surface of brainstem, and line A′, drawn along tentorium. Brainstem–vermis angle is angle between line A and line B, drawn along ventral surface of vermis. P, pons; V, cerebellar vermis.

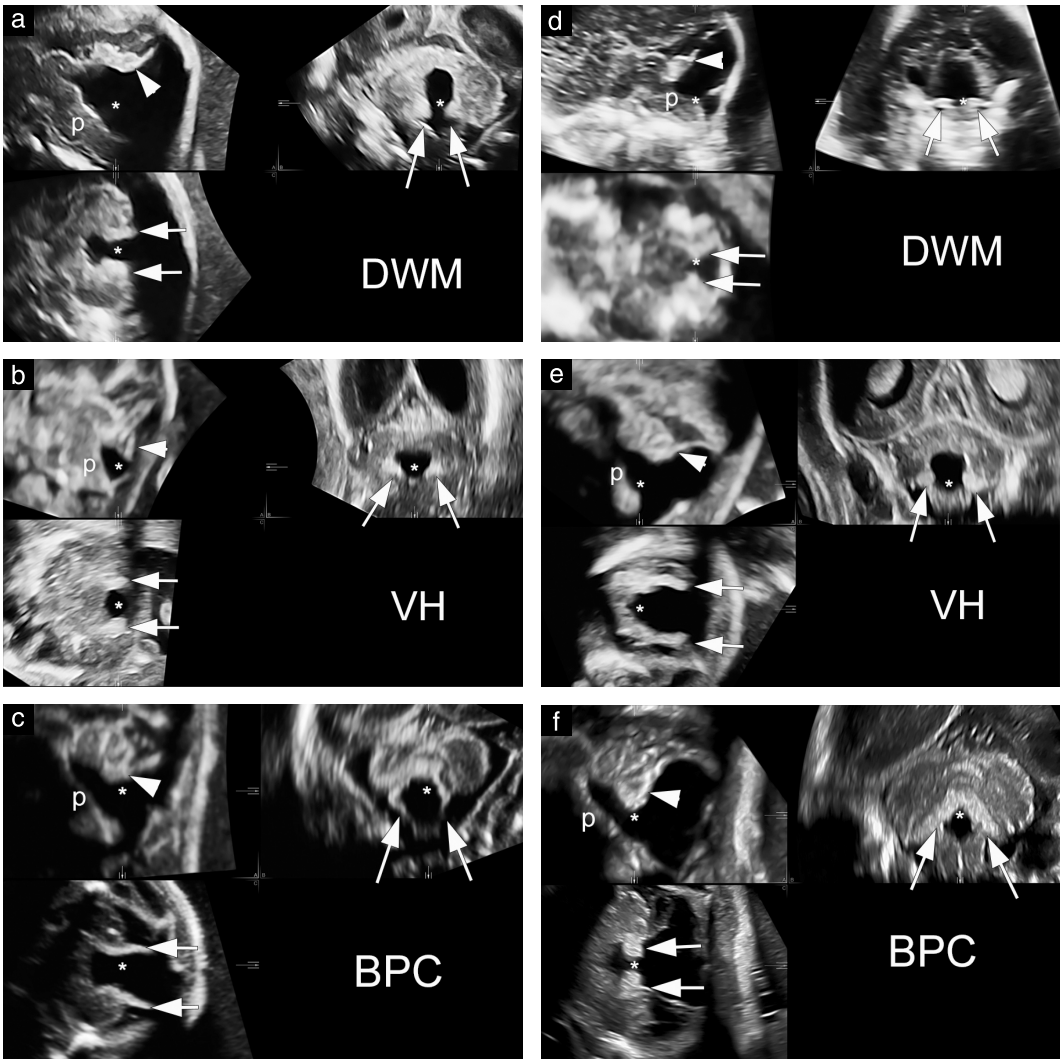

Figure 2 Transvaginal neurosonography showing position of fourth ventricular choroid plexus (4VCP, arrows) in: Dandy–Walker malformation (DWM) at 21 (a) and 22 (d) weeks' gestation, vermian hypoplasia (VH) at 18 (b) and 23 (e) weeks, and Blake's pouch cyst (BPC) at 21 (c) and 23 (f) weeks. On three-dimensional multiplanar imaging correlation, 4VCP position is assessed initially in coronal plane and, if necessary, confirmed in axial plane. In DWM and VH, 4VCP is always inferolateral in relation to cyst inlet (coronal image), whereas in BPC it is always superolateral. Position of reference marker (*) is highlighted on all three orthogonal planes. Arrowheads indicate vermis. P, pons.

and axial views (Figure 2). All images were processed and measurements taken by a single operator (D.P.). To assess the reproducibility, 17 cases were selected arbitrarily and measurements taken by a second operator (G.D.) and a second time by the first operator, with both blinded to the results of the previous evaluation.

Confirmation of the diagnosis by postmortem or neonatal MRI was available in all cases. In fetuses with more than one neurosonographic assessment, only the first was considered for the purposes of this analysis. We retrieved from the database any additional information, including karyotyping results, associated anomalies and outcome.

Statistical analysis was performed using Stata for Windows statistical software (release 13.1; Stata Corporation, College Station, TX, USA). Descriptive statistics are reported as absolute frequencies and percentages for qualitative variables and as median values and their related interquartile range (IQR) for quantitative variables. Comparison between quantitative variables was performed by Kruskal–Wallis test, and by Mann-Whitney *U*-test when comparing pairs of groups. The diagnostic performance of the variables considered was evaluated by receiver–operating characteristics (ROC) curve analysis. The area under the curve (AUC) was used as a measure of accuracy. The related 95% CI was obtained by the method of DeLong *et al.*[8]. ROC curve analysis was also used to identify the cut-off point corresponding to the optimal accuracy, i.e. corresponding to the highest value of the Youden index[9]. Repeatability was assessed by calculating the intraclass correlation coefficients (ICC) for intra- and interobserver reliability[10]. The latter was estimated by comparing measurements of the second operator with the average of the two series of available measurements from the first one. The Bland–Altman method and Pitman's test were applied to evaluate the corresponding agreement between measures, both intra- and interoperator[11,12]. All tests were two-sided and P-value < 0.05 was considered statistically significant.

RESULTS

We identified initially 142 3D volume datasets from neurosonographic examinations showing posterior fossa malformation diagnosed at our institutions between 2005 and 2017. Of these, for 62 the inclusion criteria were not met: 42 had malformations of the posterior fossa other than DWM, VH or BPC; 11 had suboptimal or only transabdominal 3D volume datasets; and nine lacked confirmation of the diagnosis. Of the remaining 80, a further 13 were excluded because they were follow-up examinations of cases already enrolled. The remaining 67, which were included in the final analysis, comprised 24 cases of DWM, 13 cases of VH and 30 cases of BPC. Of these, 18 cases with BPC and one with DWM have been reported previously[4,13]. The mean maternal age was 31 (SD, 5.1; range, 18–43) years and the mean gestational age at diagnosis was 23.6 (SD, 4.3; range, 17–36) completed gestational weeks. Number of cases with abnormal karyotype and associated anomalies and fetoneonatal outcome are shown in Table 1. Comparative genomic hybridization had been performed using the Agilent 60k microarray platform in the last three cases of DWM, and results were normal in all three; whole-genome sequencing was not performed in any case.

There was good intraobserver and interobserver reliability (ICC > 80%) for all measurements (Table 2). Bland–Altman plots are shown in Figure S1. Median (IQR) values of variables and plots of their distribution, according to the type of vermian malformation, are shown for all 67 fetuses and for the subgroup of cases diagnosed at < 23 gestational weeks in Table 3 and Figure 3. On ROC curve analysis, the parameter with the best diagnostic performance for differentiating between VH and BPC was the VA/BPD ratio, both in the whole series and in cases < 23 gestational weeks (Table 4 and Figure 4). Specifically, a VA/BPD ratio cut-off of 1.1 had sensitivity of 84.6% and specificity of 99.8% for the whole series and sensitivity of 100% and specificity of 75% for cases < 23 gestational weeks in differentiating between VH and BPC. Thus, a VA/BPD ratio > 1.1 would suggest BPC and a ratio ≤ 1.1 would suggest VH.

Table 1 Karyotype and fetoneonatal outcome in 67 cases of posterior fossa cystic malformation

Malformation	n	*Abnormal karyotype*	*Associated malformation*	*Outcome**	
				TOP	*Liveborn*
DWM	24	5 (20.8)†	11 (45.8)	20 (83.3)	4 (16.7)
VH	13	3 (23.1)‡	3 (23.1)	3 (23.1)	10 (76.9)
BPC	30	1 (3.3)§	5 (16.6)	6 (20.0)	24 (80.0)

Data are given as *n* or *n* (%). *There were no cases of intrauterine or neonatal death. †Trisomy 13 in all cases. ‡One case each of trisomy 13, trisomy 21 and del 4p. §Trisomy 21. BPC, Blake's pouch cyst; DWM, Dandy–Walker malformation; TOP, termination of pregnancy; VH, vermian hypoplasia.

Table 2 Intra- and interobserver reliability of anatomic measurements from transvaginal sonographic three-dimensional volume datasets of fetal posterior fossa

Measurement	*ICC (95% CI)*	
	Intraobserver	*Interobserver*
BTA	0.99 (0.97–1.0)	0.99 (0.96–1.0)
BVA	0.99 (0.97–1.0)	0.99 (0.97–1.0)
CCVD	0.86 (0.71–0.96)	0.89 (0.73–0.96)
APVD	0.98 (0.96–0.99)	0.84 (0.61–0.94)
VA	0.97 (0.93–0.99)	0.92 (0.79–0.97)

APVD, anteroposterior vermian diameter; BTA, brainstem–tentorium angle; BVA, brainstem–vermis angle; CCVD, craniocaudal vermian diameter; ICC, intraclass correlation coefficient; VA, vermian area.

Table 3 Anatomic measurements from transvaginal sonographic three-dimensional volume datasets of fetal posterior fossa, according to type of posterior fossa cystic malformation

Measurement	*DWM*	*VH*	*BPC*	P*	P†		
					DWM vs *VH*	*DWM* vs *BPC*	*VH* vs *BPC*
Any GA ($n = 67$)	24	13	30				
BTA (°)	43.7 (31.4–61.2)	27.7 (22.3–41.8)	25.2 (19.9–32.1)	< 0.001	NS	< 0.001	NS
BVA (°)	62.6 (41.0–78.2)	37.2 (25.3–39.6)	21.6 (12.8–35.9)	< 0.001	< 0.001	< 0.001	0.011
CCVD/BPD (%)	17.6 (14.7–19.8)	18.5 (17.3–20.5)	20.1 (18.8–22.0)	0.004	NS	0.001	NS
APVD/BPD (%)	9.7 (8.2–11.4)	11.5 (9.4–13.3)	12.8 (11.9–14.3)	< 0.001	NS	< 0.001	0.039‡
VA/BPD (%)	0.7 (0.6–1.1)	1.0 (0.8–1.1)	1.3 (1.1–1.6)	< 0.001	NS	< 0.001	< 0.001
GA < 23 weeks ($n = 47$)	17	10	20				
BTA (°)	38.2 (22.4–50.2)	23.7 (21.5–28.7)	25.4 (17.5–32.9)	0.025	NS	0.009	NS
BVA (°)	62.2 (38.3–77.2)	37.1 (25.3–39.4)	24.4 (14.3–34.3)	< 0.001	0.014	< 0.001	0.039‡
CCVD/BPD (%)	16.1 (14.2–18.5)	17.5 (16.5–19.1)	19.9 (18.4–21.6)	0.001	NS	< 0.001	0.035‡
APVD/BPD (%)	9.0 (7.6–10.5)	11.3 (9.4–12.5)	12.2 (11.8–13.3)	< 0.001	0.040‡	< 0.001	NS
VA/BPD (%)	0.6 (0.4–0.7)	0.9 (0.6–1.0)	1.2 (1.1–1.4)	< 0.001	NS	< 0.001	< 0.001

Data are given as *n* or median (interquartile range). *Comparison between all three groups by Kruskal–Wallis test. †Comparison between pairs of groups by Mann–Whitney *U*-test. ‡Not significant after Bonferroni correction for multiple-testing bias. APVD, anteroposterior vermian diameter; BPC, Blake's pouch cyst; BPD, biparietal diameter; BTA, brainstem–tentorium angle; BVA, brainstem–vermis angle; CCVD, craniocaudal vermian diameter; DWM, Dandy–Walker malformation; GA, gestational age at diagnosis; NS, not significant; VA, vermian area; VH, vermian hypoplasia.

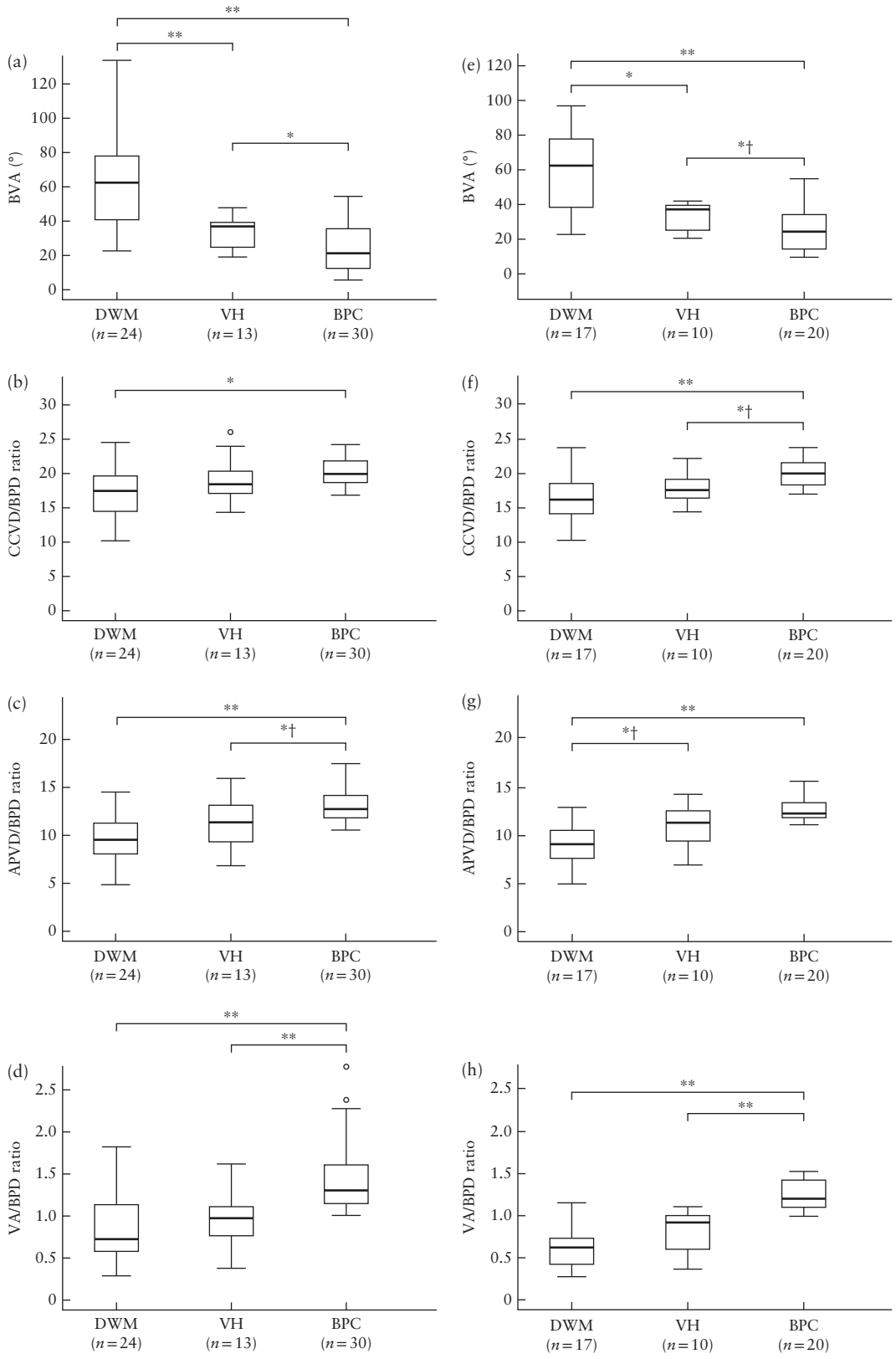

Figure 3 Box-and-whiskers plots for brainstem–vermian angle (BVA) (a,e), craniocaudal vermian diameter (CCVD)/biparietal diameter (BPD) ratio (b,f), anteroposterior vermian diameter (APVD)/BPD ratio (c,g) and vermian area (VA)/BPD ratio (d,h), in 67 fetuses diagnosed at any gestational age (a–d) and in 47 fetuses diagnosed at < 23 weeks (e–h) with posterior fossa cystic malformation, according to type (Dandy–Walker malformation (DWM), vermian hypoplasia (VH) or Blake's pouch cyst (BPC)). Boxes and internal lines show interquartile range and median, whiskers show range and circles are outliers. *$P < 0.05$. **$P < 0.001$. †Not significant after Bonferroni correction for multiple-testing bias.

Table 4 Receiver–operating characteristics curve analysis for comparison of accuracy of anatomic measurements from transvaginal sonographic three-dimensional volume datasets of fetal posterior fossa in differentiating between different types of malformation

	DWM vs *BPC*		*VH* vs *BPC*	
Diagnostic variable	*AUC (95% CI)*	P	*AUC (95% CI)*	P
Any GA ($n = 67$)		0.003		0.024
BTA	0.803 (0.673–0.932)		0.610 (0.412–0.808)	
BVA	0.912 (0.839–0.956)		0.746 (0.597–0.895)	
CCVD/BPD	0.758 (0.617–0.898)		0.664 (0.457–0.871)	
APVD/BPD	0.900 (0.809–0.991)		0.700 (0.500–0.899)	
VA/BPD	0.839 (0.718–0.960)		0.831 (0.653–1.000)	
GA < 23 weeks ($n = 47$)		0.005		< 0.001
BTA	0.753 (0.587–0.919)		0.520 (0.297–0.743)	
BVA	0.882 (0.775–0.989)		0.735 (0.550–0.920)	
CCVD/BPD	0.829 (0.687–0.972)		0.740 (0.533–0.947)	
APVD/BPD	0.953 (0.875–1.000)		0.720 (0.487–0.953)	
VA/BPD	0.959 (0.867–1.000)		0.940 (0.859–1.000)	

APVD, anteroposterior vermian diameter; AUC, area under receiver–operating characteristics curve; BPC, Blake's pouch cyst; BPD, biparietal diameter; BTA, brainstem–tentorium angle; BVA, brainstem–vermis angle; CCVD, craniocaudal vermian diameter; DWM, Dandy–Walker malformation; GA, gestational age at diagnosis; VA, vermian area; VH, vermian hypoplasia.

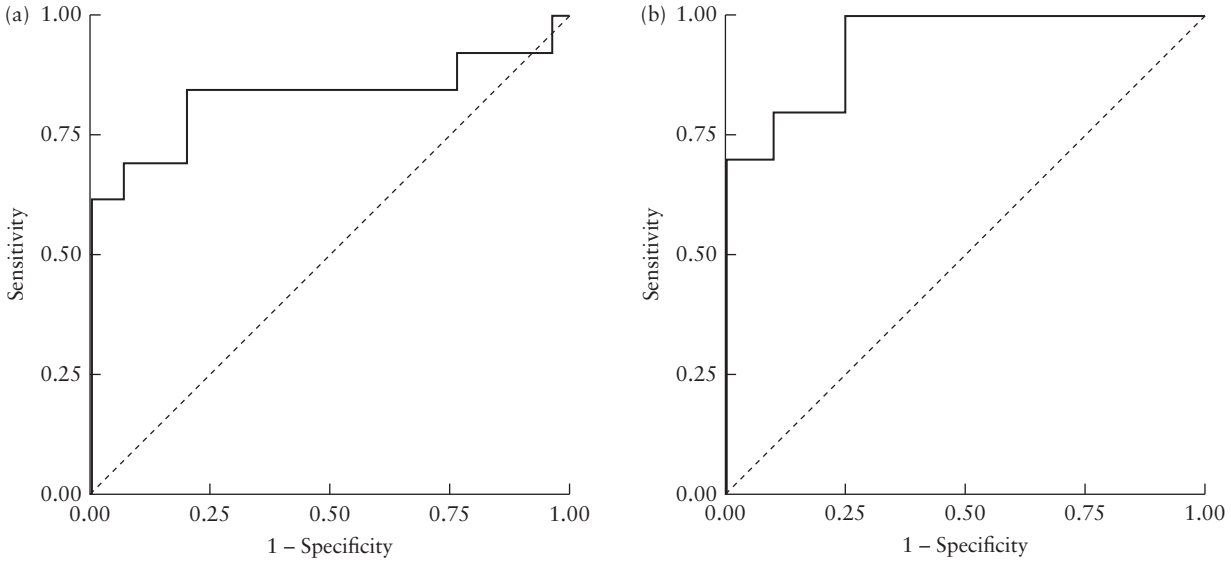

Figure 4 Receiver–operating characteristics curves for vermian area/biparietal diameter ratio in differentiating vermian hypoplasia from Blake's pouch cyst in whole study population of 67 fetuses with posterior fossa cystic malformation (a) and in subgroup of 47 cases diagnosed < 23 gestational weeks (b). Corresponding areas under the curve (95% CI) were 0.831 (0.653–1.000) and 0.940 (0.859–1.000), respectively.

With respect to the position of the 4VCP, this was down in all cases of DWM and VH, while it was up in all cases of BPC (Figure 2).

DISCUSSION

In our evaluation of hindbrain morphometry, we found that the best predictive parameter to differentiate between BPC and DWM and, especially, VH was the VA/BPD ratio (Table 3). This was also demonstrated by the ROC curve analysis, which showed, particularly in the subgroup diagnosed < 23 gestational weeks, an AUC for VA/BPD that was much larger than those for both vermian diameters as well as for BVA (Table 4 and Figure 4). In contrast, Volpe *et al.*[14], in 2012, reported that BVA was highly predictive of the type of vermian abnormality: in cases of BPC it was always < 30°, in those of DWM it was always > 45° and in those of VH it ranged between 24° and 45°; however, as these authors correctly pointed out, a limitation of their study was the sample size (31 cases overall, with seven of VH). Our study had twice as many cases with each type of anomaly and benefited from a homogeneous and high-resolution evaluation, since all cases were assessed transvaginally and with 3D multiplanar image correlation. This allowed more precise evaluation of the BVA, since visualization of the pons and brainstem is, by definition, incomplete using a transabdominal lateral approach, which was the approach used in an unspecified number of cases in the study of Volpe *et al.*[14]. We found that the VA/BPD ratio had

greater accuracy in differentiating between VH and BPC than did BVA, and that, at least in our series, there was a greater overlap between VH and BPC in BVA than there was in VA/BPD ratio, especially in the second-trimester cases (Figure 3). In conclusion, our data lead us to suggest using the VA/BPD ratio, with a cut-off value of 1.1, to differentiate between VH and BPC, regardless of gestational age.

Regarding our qualitative analysis, i.e. of 4VCP position, it should be underlined that its visualization is possible only in case of vermian rotation, because this provides a better acoustic window for imaging of the fourth ventricle and its plexus, and only using a high-resolution 3D transvaginal approach. Our decision to evaluate this structure was based on the differential pathogenesis of the analyzed cystic vermian anomalies: DWM and VH derive from abnormal development of the anterior membranous area (AMA), while the BPC represents (sometimes transient[15]) abnormal development of the posterior membranous area (PMA)[1,13,15–18]. These two structures, AMA and PMA, are separated, in Carnegie stage 14 of embryonic development, by the *plica choroidea*, which goes on to develop into the 4VCP by Carnegie stage 19 (48–51 days postovulation, gestational week 7, crown–rump length 18–20 mm)[15,16]. It is known that BPC represents a persistence of the normally transient evagination of the fourth ventricular roof, which, in the normal embryo, perforates around 12 gestational weeks to create the Magendie foramen[15,16]; as such, in BPC, the 4VCP is located on the superolateral aspect of the cyst inlet (Figure 2c,f)[8,17,18]. From necropsy and MRI studies in adults and neonates with DWM, it is known that, in this malformation, the 4VCP is found at the bottom of the generally huge cystic structure, which originates from the severely rotated vermis and extends to the brainstem, completely filling the cisterna magna; we can confirm this finding, having observed it in all of our DWM fetuses (Figure 2a,d). The low position of the 4VCP is due to the fact that, pathogenetically, DWM and its cyst derive from maldevelopment of the AMA, which is located above the *plica choroidea* and, therefore, above the choroid plexus. Along the same lines, in VH, which is also a malformation of the AMA, but generally with less hypoplasia of the vermis and less rotation, the 4VCP should also be below the cyst. Our findings support this hypothesis, with the 4VCP position being down in all cases of DWM and VH, and up in all cases of BPC (Figure 2b,e). Therefore, we propose the VA/BPD ratio and 4VPC position as the best tools with which to differentiate prenatally between DWM, VH and BPC.

It is of particular interest to speculate as to where our findings might lead. The position of the 4VCP relative to the fourth ventricle roof/cyst inlet, on one side in DWM/VH and on the other in BPC, might suggest that the development of DWM/VH or BPC may simply be a consequence of where the *plica choroidea* develops: if it develops in its proper position, then the Blake's pouch is on the roof of the fourth ventricle and, if it does not perforate in due time, BPC ensues. In contrast, if, for some reason, the *plica choroidea* develops more caudally, then – considering that Luschka foramina apparently develop much later, at around 26 gestational weeks[18] – the outpouching, which has to develop to create an outlet for the cerebrospinal fluid to the subdural space, finds the fourth ventricular roof blocked by the *plica choroidea*; therefore, it will expand above it, involving the structures related to the AMA and, consequently, leading to VH or DWM. If we follow this line of thought, then DWM and VH could be seen as the effect of ectopic (lower-than-normal) development of the *plica choroidea*. This hypothesis might also explain why, in some cases, it is only the inferior portion of the vermis that is hypoplastic; in these cases, the *plica choroidea* might have formed less caudally than it does in DWM, so that only the lowermost portion of the vermis is affected by the development of the cyst.

A strength of our study is the high-resolution transvaginal approach, which guaranteed a precise midsagittal plane in all cases; an additional advantage was the use of multiplanar image correlation, which was crucial for the assessment of 4VCP position (Figure 2). The use of multiplanar image correlation is likely to have contributed to the good reproducibility data for all measurements (Table 2); this 3D visualization mode allows contrast enhancement and increases edge sharpness, thereby reducing error in the measurements. It should be borne in mind that, since both BPD (particularly if the baby is breech) and vermian measurements may differ on transabdominal compared with transvaginal ultrasound due to the lower resolution and different approach, the cut-off reported in this study applies only to transvaginal examination.

Major limitations of this study are the relatively small number of cases, especially for the VH group, and its retrospective design. Another limitation concerns the fact that the etiology and pathogenesis of VH/vermian dysplasia is heterogeneous, with a wide range of genetic conditions involving the cerebellum and the vermis being late-onset, developing only after birth. Therefore, the findings of our analysis cannot be applied to the neonatal population. For the same reason, it is possible that the position of the 4VCP might differ in some cases from the position observed in all cases of VH in our series.

In conclusion, our data support the concept that VA/BPD ratio and 4VCP position may be used to differentiate between DWM, VH and BPC in the fetus. In our series, the position of the 4VCP had the highest accuracy, but a larger number of VH cases should be evaluated to confirm that an up position of the 4VCP indicates BPC while a down position indicates DWM or VH.

REFERENCES

1. Robinson AJ. Inferior vermian hypoplasia – preconception, misconception. *Ultrasound Obstet Gynecol* 2014; **43**: 123–136.
2. Phillips JJ, Mahony BS, Siebert JR, Lalani T, Fligner CL, Kapur RP. Dandy-Walker malformation complex: correlation between ultrasonographic diagnosis and postmortem neuropathology. *Obstet Gynecol* 2006; **107**: 685–693.
3. Klein O, Pierre-Kahn A, Boddaert N, Parisot D, Brunelle F. Dandy-Walker malformation: prenatal diagnosis and prognosis. *Childs Nerv Syst* 2003; **19**: 484–489.

4. Paladini D, Volpe P. Posterior fossa and vermian morphometry in the characterization of fetal cerebellar abnormalities: a prospective three-dimensional ultrasound study. *Ultrasound Obstet Gynecol* 2006; **27**: 482–489.
5. Siebert JR. A Pathological Approach to Anomalies of the Posterior Fossa. *Birth Defects Res (Part A)* 2006; **76**: 674–684.
6. International Society of Ultrasound in Obstetrics & Gynecology Education Committee. Sonographic examination of the fetal central nervous system: guidelines for performing the 'basic examination' and the 'fetal neurosonogram'. *Ultrasound Obstet Gynecol* 2007; **29**: 109–116.
7. Malinger G, Ginath S, Lerman-Sagie T, Watemberg N, Lev D, Glezerman M. The fetal cerebellar vermis: normal development as shown by transvaginal ultrasound. *Prenat Diagn* 2001; **21**: 687–692.
8. DeLong ER, DeLong DM, Clarke-Pearson DL. Comparing the areas under two or more correlated receiver operating characteristic curves: a nonparametric approach. *Biometrics* 1988; **44**: 837–845.
9. Pepe MS. The statistical evaluation of medical tests for classification and prediction. Oxford University Press: Oxford, UK, 2003.
10. Shrout PE, Fleiss JL. Intraclass correlations: uses in assessing rater reliability. *Psychol Bull* 1979; **86**: 420–428.
11. Bland JM, Altman DG. Statistical methods for assessing agreement between two methods of clinical measurement. *Lancet* 1986; **327**: 307–310.
12. Bartlett JW, Frost C. Reliability, repeatability and reproducibility: analysis of measurement errors in continuous variables. *Ultrasound Obstet Gynecol* 2008; **31**: 466–475.
13. Paladini D, Quarantelli M, Pastore G, Sorrentino M, Sglavo G, Nappi C. Abnormal or delayed development of the posterior membranous area of the brain: anatomy, ultrasound diagnosis, natural history and outcome of Blake's pouch cyst in the fetus. *Ultrasound Obstet Gynecol* 2012; **39**: 279–287.
14. Volpe P, Contro E, De Musso F, Ghi T, Farina A, Tempesta A, Volpe G, Rizzo N, Pilu G. Brainstem-vermis and brainstem-tentorium angles allow accurate categorization of fetal upward rotation of cerebellar vermis. *Ultrasound Obstet Gynecol* 2012; **39**: 632–635.
15. Blake JA. The roof and lateral recesses of the fourth ventricle, considered morphologically and embryologically. *J Comp Neurol* 1900; **10**: 79–108.
16. Wilson JT. On the nature and mode of origin of the foramen of Magendie. *J Anat* 1936–1937; **71**: 423–428.
17. Tortori-Donati P, Fondelli MP, Rossi A, Carini S. Cystic malformations of the posterior fossa originating from a defect of the posterior membranous area. Mega cisterna magna and persisting Blake's pouch: two separate entities. *Childs Nerv Syst* 1996; **12**: 303–308.
18. Brocklehurst G. The development of the human cerebrospinal fluid pathway with particular reference to the roof of the fourth ventricle. *J Anat* 1969; **105**: 467–475.

SUPPORTING INFORMATION ON THE INTERNET

The following supporting information may be found in the online version of this article:

Figure S1 Bland–Altman plots for evaluation of intraoperator (left panels) and interoperator (right panels) agreement for analyzed variables. APVD, anteroposterior vermian diameter; BTA, brain–tentorium angle; BVA, brain–vermis angle; CCVD, craniocaudal vermian diameter; VA, vermian area.